Excited-State Behavior of 2-(4′-Pyridyl)benzimidazole in Aqueous Solution: Proton-Transfer Processes and Dual Fluorescence

Mercedes Novo, Manuel Mosquera,* and Flor Rodríguez Prieto*

Departamento de Química Física, Facultade de Química, Universidade de Santiago, E-15706 Santiago de Compostela, Spain

Received: February 23, 1995; In Final Form: July 7, 1995[⊗]

The excited-state acid−base behavior of 2-(4′-pyridyl)benzimidazole in aqueous solution has been studied over a wide range of acidity by UV absorption and fluorescence spectroscopy. The species detected in the lowest electronically excited singlet state turned out to be identical to those of the ground state: the anion A, the neutral molecule N, the monocation C protonated at the benzimidazole N3, the monocation T protonated at the pyridyl nitrogen, and the dication D. Nevertheless, the strong increase in the basicity of the pyridyl nitrogen atom in the excited state induces different excited-state proton-transfer processes. The dual fluorescence of 4PBI at neutral pH is explained by the protonation of N* to give T*. On the basis of the steady-state data together with the fluorescence decay measurements at several acidities, a mechanism is proposed to explain the acid−base behavior of 4PBI in the first excited singlet state.

Introduction

This paper continues our series[1−3] on the ground- and excited-state acid−base behavior of 2-pyridylbenzimidazoles. As previously reported,[2] 2-pyridylbenzimidazoles show an interesting acid−base behavior due to the presence of two nitrogen atoms which may compete for protons in these compounds. Thus, while protonation of 2-(2′-pyridyl)benzimidazole (2PBI) and 2-(3′-pyridyl)benzimidazole (3PBI) in the ground state occurs only at the benzimidazole nitrogen atom N3, their isomer 2-(4′-pyridyl)benzimidazole (4PBI) protonates both at the benzimidazole N3 and at the pyridyl nitrogen, leading to the existence of two monocations in equilibrium in the ground state.

As is well known,[4−7] the excited-state acid−base properties of molecules may differ considerably from those in the ground state, leading to interesting proton-transfer processes. To investigate such properties of 2-pyridylbenzimidazoles, we have studied the influence of acidity on their fluorescence spectra. We reported[1] the occurrence of various photoinduced proton-transfer processes in 2PBI, leading to the formation of a new species in the excited state, the monocation protonated at the pyridyl nitrogen (T*). This species was however not detected for 3PBI.[3] Study of the quaternary salt 2-(1-methyl-4-pyridinio)benzimidazole iodide (4PBIQS) provided specific information about the effects of a positive charge at the pyridyl nitrogen on the fluorescence spectra of these compounds.[3] Moreover, due to the very similar structure of 4PBIQS compared to that of 4PBI protonated at the pyridyl nitrogen (4PBIQS having a methyl group where that monocation of 4PBI has its additional hydrogen), the quaternary salt has been a very helpful model for the interpretation of the complex acidity dependence of the fluorescence spectra of 4PBI, the objective of the present work.

Previously,[2] it was shown that five different forms of 4PBI are involved in its ground-state acid−base equilibria; the anion A, the neutral molecule N, the monocation C protonated at the benzimidazole N3, the monocation T protonated at the pyridyl nitrogen, and the dication D. Those species are shown in the lower part of Scheme 1, together with the corresponding acid−base equilibria. Spectrophotometric titration determined the acidity constant K_{NA} ($pK_{NA} = 10.78 \pm 0.02$) and the macroscopic acidity constants K_1 and K_2 ($pK_1 = 1.96 \pm 0.02$, $pK_2 = 4.47 \pm 0.01$), which are related to the microscopic acidity constants shown in Scheme 1 by

$$K_1 = K_{DC} + K_{DT}$$

$$\frac{1}{K_2} = \frac{1}{K_{CN}} + \frac{1}{K_{TN}}$$

By comparing the behavior of 4PBI with that of the quaternary salt 4PBIQS, the values of the microscopic acidity constants of 4PBI could be estimated to be $pK_{DC} \simeq pK_{DT} \simeq 2.26$ and $pK_{CN} \simeq pK_{TN} \simeq 4.17$, indicating a remarkably equal basicity of the benzimidazole nitrogen atom N3 and the pyridyl nitrogen atom in the ground state of 4PBI. This implies that both monocations C and T are always present in about the same proportions in aqueous solutions. It is interesting to know whether this behavior changes in the excited state.

Experimental Section

4PBI was synthesized as previously described[2] and was purified by repeated recrystallization from ethanol/water followed by column chromatography. Acidity was varied using perchloric acid and sodium hydroxide, and ionic strength was controlled with sodium perchlorate, being 0.1 mol dm^{-3} in all the solutions except those for lifetime measurements and those with $[HClO_4] > 0.1$ mol dm^{-3}, whose ionic strength was the concentration of the acid. The concentration of 4PBI in the solutions was $\sim 4 \times 10^{-5}$ mol dm^{-3} for the absorption spectra and $\sim 7 \times 10^{-6}$ mol dm^{-3} for the fluorescence spectra. All chemicals were obtained from Merck p.a.

Fluorescence spectra were normally recorded on a Perkin-Elmer 650-40 spectrofluorometer. Emission spectra were corrected for the wavelength dependence of the sensitivity of the detection system,[1] while excitation spectra are uncorrected. Some spectra were recorded in a Spex Fluorolog 2 spectrofluorometer, where excitation spectra could be corrected. All measurements were performed at a constant temperature of 25 °C without prior deoxygenation of the solutions. Quenching by oxygen was proved to be negligible. At acidities lower than $[HClO_4] = 0.01$ mol dm^{-3}, the proton concentration was

[⊗] Abstract published in *Advance ACS Abstracts*, September 1, 1995.

0022-3654/95/2099-14726$09.00/0

SCHEME 1

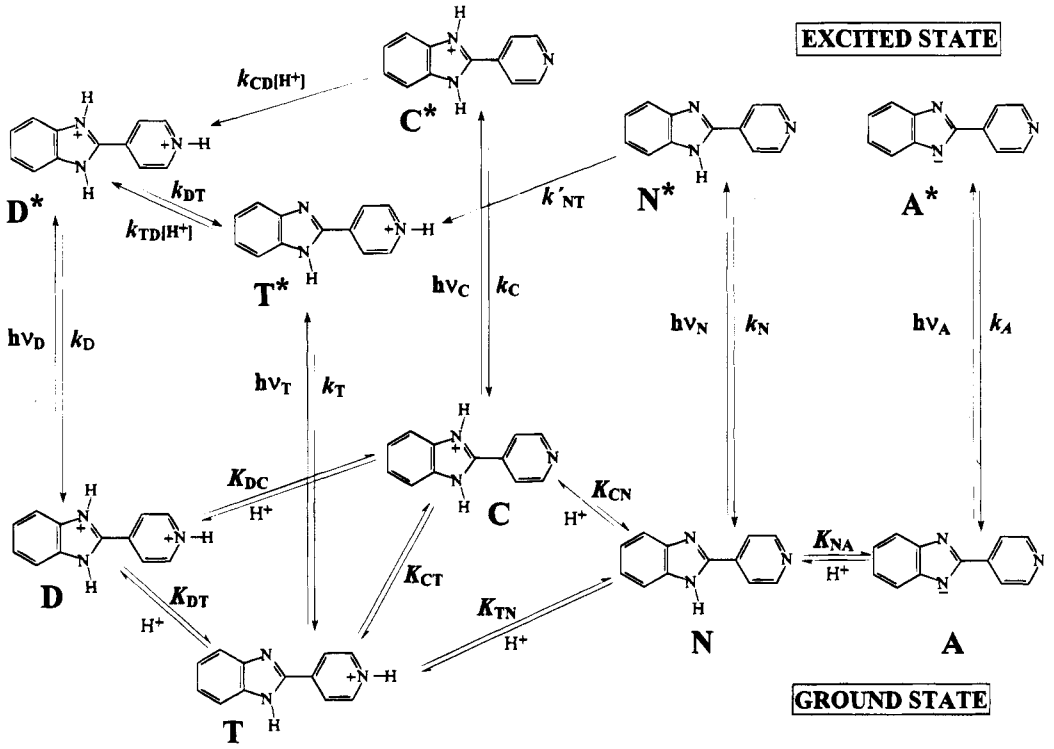

determined by measuring the pH with a Radiometer PHM82 pH meter equipped with a type B combined electrode. The fluorescence lifetimes were measured using the time-correlated single-photon-counting technique with the same apparatus as in ref 1 and also with an Edinburgh Instruments CD900 fluorescence lifetime spectrometer. A N_2- or H_2-filled nanosecond flashlamp from Edinburgh Instruments was used to excite the samples.

Results

The fluorescence excitation and emission spectra of 4PBI in neutral media are shown in Figure 1c,d. Dual fluorescence is observed with two overlapped emission bands. The high-energy band (blue band) shows a normal Stokes shift with respect to the excitation spectrum, which is practically independent of the emission wavelength, whereas the low-energy band (red band) has a very large Stokes shift. The ratio of the intensities of the two bands remains constant at any excitation wavelength. The intensities of both bands decrease as the pH is increased (Figure 2a,b). In the neighborhood of pH 13, the blue band disappears while the red band has a very low intensity and is shifted to lower wavenumbers. At that high pH, the excitation spectrum of 4PBI is shifted toward lower energies with respect to that in neutral media (results not shown).

At about pH 3, both emission and excitation spectra become strongly dependent on the monitoring wavelength (Figure 3). Two emission bands analogous to those in neutral media are observed at excitation wavelengths less than 340 nm, whereas excitation at longer wavelengths induces a single emission band with a maximum around 19 500 cm^{-1}. The ratio of the intensities of the two emission bands depends strongly on the excitation wavelength. Two different excitation spectra are obtained when monitoring at the emission wavelengths of 380 nm (blue band) and 550 nm (red band). The excitation spectrum of the blue band is similar to that obtained in neutral media and that of the red band, at lower wavenumber, shows a normal Stokes shift with respect to the red emission band (Figure 3).

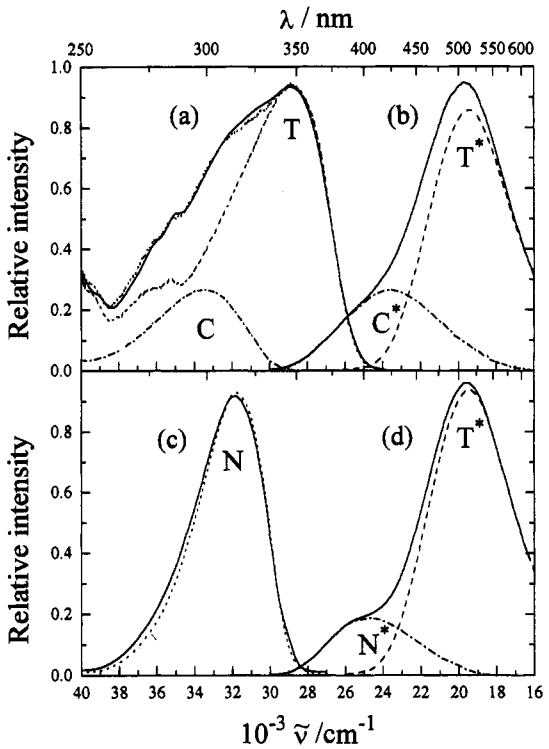

Figure 1. (a) Absorption spectrum of 4PBI at pH 3.05 (—) and corrected excitation spectra at the same pH for 380-nm emission (— • —, label C) and 550-nm emission (— —, label T). The dotted line shows the theoretical absorption spectrum obtained by fitting a linear combination of the two excitation spectra. The intensity of the excitation spectra represent their contribution to the absorption spectrum. (b) Corrected fluorescence spectrum of 4PBI at pH 2.94 and 325-nm excitation (—) together with the individual contributions of the fluorescence of C* (— • —) and T* (— —). The spectrum of T* was measured experimentally with excitation at 349 nm. (c) Normalized uncorrected excitation spectra of 4PBI at pH 7.21 with 390-nm emission (—) and 490-nm emission (• • •). (d) Corrected emission spectrum of 4PBI at pH 7.47 and 315-nm excitation (—) together with the individual contributions of the fluorescence of N* (— • —) and T* (— —).

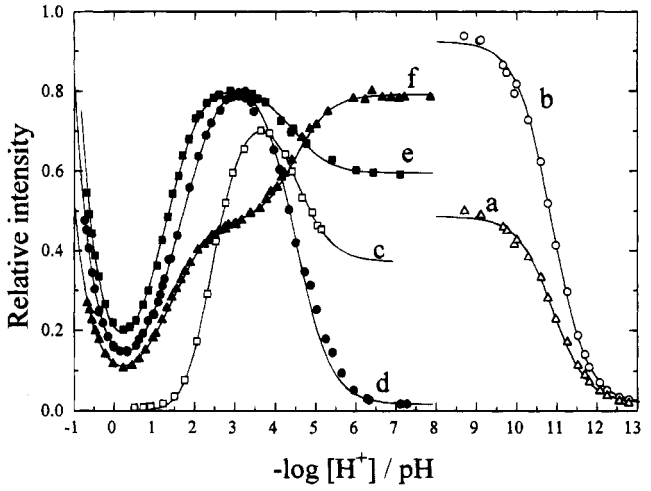

Figure 2. Fluorescence intensities of 4PBI plotted against pH. (a) λ_{em} = 380 nm, λ_{ex} = 315 nm; (b) λ_{em} = 490 nm, λ_{ex} = 315 nm; (c) λ_{em} = 390 nm, λ_{ex} = 325 nm; (d) λ_{em} = 490 nm, λ_{ex} = 349 nm; (e) λ_{em} = 490 nm, λ_{ex} = 325 nm; (f) λ_{em} = 490 nm, λ_{ex} = 304 nm. Each series of data has its own relative scale. The solid curves are the result of fitting the theoretical equations derived from the mechanism in Scheme 1 to the experimental data.

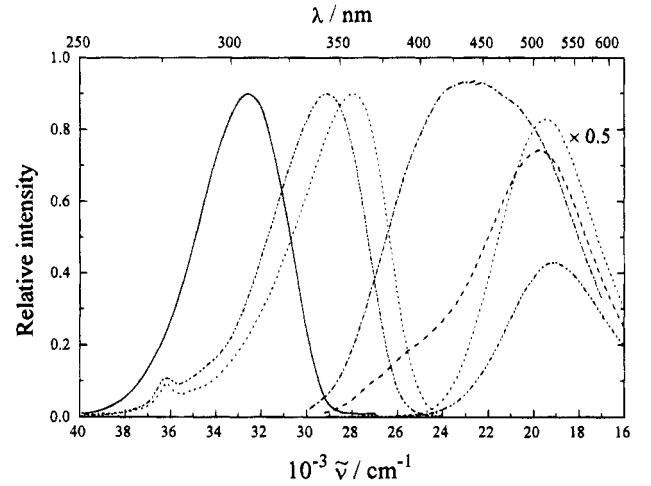

Figure 3. Uncorrected 4PBI excitation spectra for pH 3.00 and 380-nm emission (—), pH 3.00 and 550-nm emission (• • •), and [H^+] = 3.5 mol dm^{-3} and 550-nm emission (— • • —). Corrected 4PBI emission spectra for pH 3.00 and 304-nm excitation (— • —), pH 3.02 and 325-nm excitation (— —), pH 3.09 and 349-nm excitation (• • •), and [H^+] = 3.5 mol dm^{-3} and 325-nm excitation (— • • —).

At higher acidities, when the dication D is the only species that exists in the ground state, a single emission band with a maximum around 19 000 cm^{-1} is observed at any excitation wavelength (Figure 3). The corresponding excitation spectrum coincides with the absorption spectrum of species D.[2]

For the blue emission band in neutral-to-acidic media and at any excitation wavelength, the fluorescence intensity increases with acidity to reach a maximum at about pH 3.5 and wanes thereafter to disappear at [H^+] > 0.1 mol dm^{-3} (Figure 2c). Conversely, the variation of the red-band fluorescence intensity with acidity depends on the excitation wavelength, as shown in Figure 2d–f. An increase of the red-band intensity is observed at a fixed high acidity ([H^+] ≃ 1 mol dm^{-3}) when the concentration of $NaClO_4$ is increased, showing the same linear dependence on [$NaClO_4$] as was found for the quaternary salt 4PBIQS.[3]

Turning to the fluorescence decay measurements, biexponential decays were measured at 316-nm excitation and 380-nm emission in the pH range 7–3. At neutral pH a species

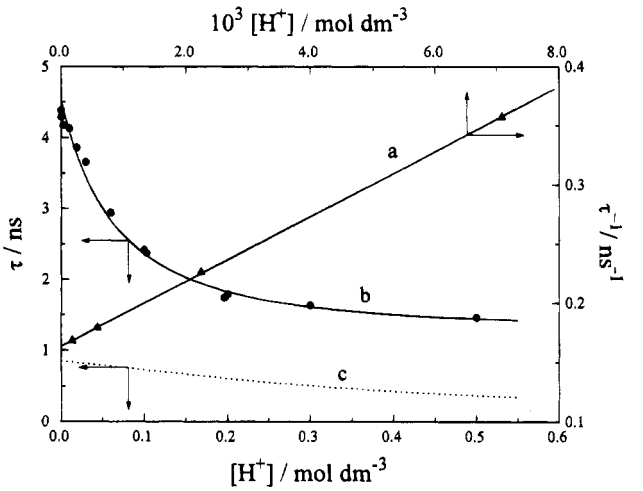

Figure 4. (a) [H^+] dependence of the reciprocal of the lifetime of 380-nm fluorescence with excitation at 316 nm. The solid line results of fitting the Stern–Volmer equation to the experimental data. (b and c) [H^+] dependence of the lifetime of 520-nm fluorescence with excitation at 349 nm. The solid line results of fitting the corresponding theoretical equation (eq 3 with minus sign) to the experimental data and the dashed line is obtained by substituting the fitted parameters in the theoretical equation for τ_1 (eq 3 with plus sign).

with a lifetime of 0.2 ns is the major contributor to the emission (99.9%). The amplitude of this component of the decay decreases with increasing acidity, while the contribution of a second species with a lifetime of 6.0 ns increases. At pH < 3 the fluorescence decay becomes monoexponential. The measured lifetimes decrease as acidity increases, showing a linear variation of τ^{-1} with the proton concentration (Figure 4a). Another series of fluorescence decay measurements was performed at 349-nm excitation and 520-nm emission in the range from pH 4 to [H^+] = 0.5 mol dm^{-3}. These decays were all monoexponentional with a lifetime of 4.3 ns at pH 4 which decreases at higher acidities (Figure 4b), but whose plot of τ^{-1} versus the concentration of protons is not linear.

Discussion

Fluorescence Spectra. In neutral media 4PBI shows two overlapped emission bands (Figure 1d) whose maxima are separated by about 5000 cm^{-1}, being attributable to two different excited species. Since the excitation spectra of the two bands are virtually identical (Figure 1c), it must be concluded that both species have the same ground-state precursor, the neutral species N, which predominates at neutral pH and whose low-energy absorption band[2] coincides with the excitation spectrum.[8] Moreover, since the blue band has a "normal" Stokes shift with respect to the absorption band and resembles the only fluorescence band observed in nonaqueous solvents,[9,10] it may be attributed to the excited neutral species N*, whereas the red band, which shows a very large shift, may be due to a new species formed in the excited state from species N*. Taking into account the great resemblance of this behavior to that of 2PBI in neutral media,[1] the red band can be attributed as in the latter to the monocation protonated at the pyridyl nitrogen T*, which is formed by protonation of the neutral species N*. Both emission bands decline as the pH is increased from pH 7 to 13 (Figure 2a,b) showing a red shift in very basic media together with a shift of the excitation spectrum toward lower energies. This behavior is typical of benzimidazoles[11,12] and also 2-pyridylbenzimidazoles[1,3] in basic media, and likewise it may be explained on the basis of the formation of the anion A, a species with a very low fluorescence quantum yield whose absorption spectrum is red shifted with respect to that of N.[2]

In neutral-to-acidic media the ratio of the intensities of the two emission bands becomes dependent on the excitation wavelength, as the excitation spectra of the two bands differ (Figure 3). At pH 3 the peak of the blue-band excitation spectrum lies at much higher energies than that of the red band. This shows the presence of two different ground-state species responsible for each of the emission bands, confirming the interpretation given in previous work[2] for the broad absorption spectrum of 4PBI at pH 3 due to the presence of the two monocations C and T. In fact, the absorption spectrum can be satisfactorily reproduced by a linear combination of the two corrected excitation spectra (Figure 1a). The slight differences observed between the experimental absorption spectrum (solid line) and the fitted combination spectrum (dotted line) are attributed to the low percentages of dication and neutral form existing at pH 3 due to the proximity of the values of pK_1 and pK_2. In this way, the individual absorption spectra of both monocations could be determined. This is not possible by absorption measurements. In agreement with this interpretation, the high-energy excitation band and the blue emission band must be attributed to the monocation protonated at the benzimidazole N3, C*, whose absorption and fluorescence spectra are very similar to those of N*, whereas the low-energy excitation band and the red emission band are due to the monocation protonated at the pyridyl nitrogen, T*, which resembles the photophysical behavior of the quaternary salt 4PBIQS.[3]

The individual emission spectrum of species T* is obtained experimentally at pH 3 with excitation at 349 nm (Figure 3) since species C does not absorb at that wavelength. The fluorescence quantum yield of T* is 0.12, determined by using quinine sulfate in 1 N H_2SO_4 as standard (quantum yield 0.546).[13] The emission spectrum of C* can be calculated by taking the difference between the experimental spectrum measured with excitation at 325 nm and that of T*, previously normalized at 625 nm (Figure 1b). Once the emission spectra of C* and T* are known, we can show that the experimental spectra at any excitation wavelength can be obtained by adding the appropriate contributions of the individual spectra. The determination of the absorption spectra of both monocations (Figure 1a) allowed the fluorescence quantum yield of C* to be determined, resulting in a value of 0.06, of the same order as that for 2PBI (0.09)[1] and 3PBI (0.03).[3] This quantum yield proved to be independent of the excitation wavelength.

We used the same procedure in order to verify the hypothesis that the 4PBI emission spectrum at neutral pH is composed of contributions from the individual spectra of the species N* and T*. Subtraction of the spectrum of T* obtained in acid media from the experimental emission spectrum at pH 7.47, previously normalized at long wavelengths, yields a well-shaped band for N* that resembles those of the other 2-pyridylbenzimidazoles[1,3] (Figure 1d). This result supports the photoinduced formation of the monocation T* from N* as explanation for the dual fluorescence of 4PBI at neutral pH . The ratio between the integrals of the contributions of T* and N* to the experimental emission spectrum at neutral pH has a value $R_{T/N} = 3.24$, about 20 times higher than that measured for 2PBI.[1] The fluorescence quantum yield of N* was 0.0022, about 15 times lower than that of the neutral species of 2PBI.[1]

At acidities higher than pH 3, the blue band wanes (Figure 2c) while the intensity of the red band decreases with increasing acidity up to $[H^+] \simeq 0.7$ mol dm^{-3} and increases thereafter (Figure 2d–f). In this acidity range, the red-band excitation spectrum shifts toward higher energies, resembling the behavior of the absorption spectrum,[2] whereas the emission spectrum shows a slight red shift (Figure 3). Since it is known from the absorption measurements that protonation of the two ground-state monocations, C and T, occurs at these acidities to give a dication D with a low-energy absorption band shifted toward higher energies, the excitation spectrum obtained at high acidities has to be attributed to species D, which predominates at $[H^+] > 0.1$ mol dm^{-3}. Despite the small overlap between the excitation and the emission bands, the excited-state dication D* must be responsible for the slightly red-shifted emission spectrum, this assignment being in agreement with the interpretation of the 4PBIQS fluorescence spectra at high acidities, a species which shows analogous photophysical behavior.[3] The large Stokes shift observed for these dications may be due to an excited-state conformational change toward planarity by torsion around the interannular bond, detected in various 2-phenylbenzazoles.[14,15]

Concerning the increase of the red-band intensity at acidities higher than $[H^+] \simeq 0.7$ mol dm^{-3}, this is also observed when increasing the concentration of $NaClO_4$ at a fixed proton concentration (results not shown) as in the case of the quaternary salt 4PBIQS.[3] It is likewise attributed to an effect of the medium on the fluorescence quantum yield of D*.

Table 1 summarizes the absorption and fluorescence maxima of the different forms of 4PBI as well as their fluorescence quantum yields.

TABLE 1: Absorption and Fluorescence Maxima and Fluorescence Quantum Yields of the Various Protonated and Deprotonated Forms of 4PBI

species	$\tilde{\nu}_{max}$(abs)/cm^{-1}	$\tilde{\nu}_{max}$(fl)/cm^{-1}	ϕ_{fl}
D	30 000[a]	19 000	
C	34 500	23 500	0.06
T	28 600	19 500	0.12
N	32 500[a]	24 700	0.0022
A	31 000[a]		

[a] Reference 2.

TABLE 2: Ground- and Excited-State Acidity Constants of the Various Acid–Base Equilibria of 4PBI and Estimated Values of the Excited-State Deprotonation Rate Constants Assuming That the Protonation Rate Constants Are in the Diffusion-Controlled Limit

equilibrium	pK_a[a]	pK_a*[b]	deprotonation rate constants/s^{-1}
D* ⇌ C* + H$^+$	2.26	9.9	$k_{DC} \simeq 6$
D* ⇌ T* + H$^+$	2.26	1.0[c]	$k_{DT} \simeq 5 \times 10^9$
C* ⇌ N* + H$^+$	4.17	4.8	$k_{CN} \simeq 8 \times 10^5$
T* ⇌ N* + H$^+$	4.17	14	$k_{TN} \simeq 1 \times 10^{-3}$
N* ⇌ A* + H$^+$	10.78	7.5	$k_{NA} \simeq 2 \times 10^3$

[a] Reference 2. [b] Calculated by using the Förster cycle method. [c] This value coincides with the pK_a* calculated from dynamic measurements of k_{DT} and k_{TD} (see Table 3).

Table 2 summarizes the ground- and excited-state acidity constants of the various acid–base equilibria of 4PBI and estimated values of the excited-state deprotonation rate constants assuming that the protonation rate constants are in the diffusion-controlled limit.

Acid–Base Processes in the Excited State. As a first approximation to the excited-state acid–base behavior of 4PBI, the pK_a* of the corresponding acid–base equilibria in the excited state were calculated by the Förster cycle method[5] (Table 2). Due to the lack of distinct 0–0 transitions in the spectra, their frequencies were estimated from the mean of absorption and fluorescence peak values, except for the pK^*_{NA} which was calculated from the absorption peaks since A* has a very low fluorescence quantum yield. These estimations, together with the fact that the values of the microscopic ground-state acidity constants are also not exactly known, introduce some uncertainty in the values obtained. The pK_a* listed in Table 2 can therefore differ by 2 or 3 units from the true values and should be viewed with due caution. The values of pK_{DT} and pK_{CN} are close in the ground and the excited state, indicating similar basicity of the benzimidazole nitrogen atom N3 in both states. The high values obtained for pK^*_{DC} and pK^*_{TN} indicate a big increase in

the basicity of the pyridyl nitrogen in the excited state. A similar increase is also observed for the ortho isomer 2PBI,[1] but not for the meta isomer 3PBI.[3]

From the several acid–base processes that may take place among the five different forms of 4PBI in the excited state, only those that are fast enough to compete with the deactivation of the excited species will be observed. According to Eigen's theory of proton transfer,[16] the protonation rate constants k_{CD}, k_{TD}, k_{NC}, k_{NT}, and k_{AN} should be of the same order as the diffusion-controlled limit (5×10^{10} dm^3 mol^{-1} s^{-1}), and with this assumption, the corresponding deprotonation rate constants can be estimated from the Förster-cycle pK_a* (Table 2). In view of the values obtained, only k_{DT} would be large enough to compete with the deactivation of the excited species, whose rate constants are shown by the measured lifetimes to be greater than 10^8 s^{-1} in all cases. On the other hand, the rate of the protonation processes is determined by the concentration of protons and, since the species N* and A* exist only at pH > 3, it can be concluded that their protonation processes (with effective rates $k_{NC}[H^+]$, $k_{NT}[H^+]$, and $k_{AN}[H^+]$) are not fast enough in comparison with the deactivation processes of those species and will not be observed. Nevertheless, the experimental emission spectra of 4PBI in neutral-to-basic media show dual fluorescence, which has been attributed to the emission of both species N* and T* (Figure 1d), the latter being formed by a photoinduced proton-transfer process from N*. Since not enough protons are present in those media to allow the protonation of N*, the possibility should be considered (as in the case of 2PBI[1]) that molecules of water protonate species N* in a process of rate k'_{NT} (including the concentration of water) which competes with the deactivation rate of N*. A recently published compilation of data for the excited-state protonation processes of several aromatic amines by water[7] supports our interpretation, since values of protonation rate constants of $(2-3) \times 10^8$ s^{-1} are reported for aromatic amines with pK_a* around 12.5. Although for these amines the reverse rate constants have values from 5×10^9 dm^3 mol^{-1} s^{-1} up to the diffusion-controlled limit, which can also be expected for the monocation T* of 4PBI, the rate of the deprotonation process is determined by the concentration of species OH^-, being only fast enough to compete with the deactivation of the excited species in quite basic media. Therefore, under the experimental conditions studied for 4PBI the reverse process of rate $k'_{TN}[OH^-]$ will not be observed.

Finally, the tautomerization process between C* and T* remains to be considered, whose equilibrium constant K^*_{CT} is about 10^9 according to the estimated pK_a* values (Table 2). Such a large value of K^*_{CT} indicates that the tautomerization process of C* to give T* is highly favored, as in the case of the isomer 2PBI.[1] Two parallel tautomerization processes C* → T* were observed in 2PBI: (i) protonation of C* followed by deprotonation of D*, and (ii) a one-step concerted reaction in which one or more water molecules could be involved allowing the simultaneous deprotonation of benzimidazole and protonation of the pyridyl group. The occurrence of process (i) was proved by the observation of a quenching of C* fluorescence by protons which partially yielded T*. On the other hand, process (ii) manifested itself in the dual fluorescence observed at pH 3, when only monocation C* exists in the ground state and the quenching of C* is insignificant due to the low concentration of protons. In the case of 4PBI, quenching of the two excited monocations by protons occurs and these processes have rate constants, k_{CD} and k_{TD}, which are close to the diffusion-controlled limit, as will be demonstrated below. 4PBI also shows dual fluorescence at pH 3, conditions under which the quenching of C* by protons is insignificant. Nevertheless, it must be taken into account that tautomer T of 4PBI exists in the ground state together with C and that it is impossible to excite the latter selectively, as shown in Figure 1a. Therefore, in order to examine whether the concerted tautomerization C* → T* is efficient in 4PBI, the fluorescence quantum yields of T* at different excitation wavelengths at which C also absorbs were determined on the basis of the decomposition of the experimental absorption spectrum at pH 3 in Figure 1a. The values obtained at 304, 315, 325, and 360 nm were identical within the experimental error. This result proves that no conversion of C* to T* takes place at pH 3 and that 4PBI does not show concerted tautomerization. This difference in behavior with respect to 2PBI may be due to the large distance in 4PBI between the two atoms involved in the proton transfer, the benzimidazole nitrogen atom N3 and the pyridyl nitrogen atom. In the case of 2PBI both nitrogen atoms are very close, so that a concerted process of protonation and deprotonation can easily take place with the involvement of only one water molecule, the structure of the complex formed by hydrogen bonds being similar to that proposed to explain the decrease of the fluorescence quantum yield of 2PBI in the presence of alcohols:[9,10]

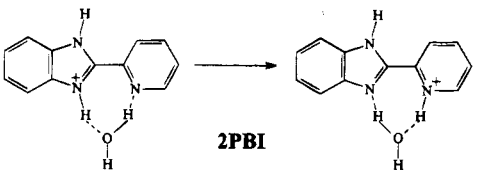

It could even be possible that the proton transfer is intramolecular, without the involvement of a water molecule. In that case, a five-membered cyclic system would be formed by a hydrogen bond N–H···N which would allow the intramolecular proton transfer to occur. None of these possibilities is plausible for 4PBI due to the large distance between the nitrogen atoms. Therefore, a concerted process would be possible only with the involvement of several water molecules and that makes the process very unlikely to be efficient, as experimentally observed.

Taking into account the above considerations, a mechanism is proposed to explain the acid–base behavior of 4PBI in the excited state, as shown in Scheme 1. Each process expected to occur in the excited state is denoted by its effective rate. The deactivation rate constants of the excited species are represented by k_A, k_N, k_C, k_T, and k_D. The ground-state acid–base equilibria are represented by their acidity constants. To prove whether this mechanism is in keeping with the experimental data, a quantitative analysis of both time-resolved and steady-state fluorescence data is performed, in which also the rate constants of the different excited-state proton-transfer processes are calculated.

Quantitative Analysis. Acording to the mechanism proposed (Scheme 1), the pH dependence of the fluorescence intensity of the two emission bands in neutral-to-basic media is due to the acid–base equilibrium between N and A in the ground state.[17] Analysis of the experimental data (Figure 2a,b) yields the following values of pK_{NA}: 10.89 for the data at 380 nm and 10.88 for the data at 490 nm, in good agreement with the value determined from absorption measurements (10.78).[2]

In neutral-to-acidic media we derived from the mechanism proposed above an equation relating emission intensity at a given wavelength to proton concentration.[18] In this equation, the effect of the medium on the quantum yield of D* was quantified by assuming a linear variation of the fluorescence intensity of D* with the concentration of acid, as in the case of 4PBIQS.[3] The

TABLE 3: Rate Constants for the Various Processes of 4PBI in the First Excited Singlet State in Aqueous Solution

reaction rate constants/ns^{-1}	deactivation rate constants/ns^{-1}	radiative deactivation rate constants/ns^{-1}
$k'_{NT} = 0.27$	$k_N = 4.7$	$k_{rN} = 0.01$
$k_{CD} = (27.5 \pm 0.2)$ dm^3 mol^{-1}	$k_C = 0.163 \pm 0.003$	$k_{rC} = 0.01$
$k_{TD} = (4.0 \pm 0.3)$ dm^3 mol^{-1}	$k_T = 0.221 \pm 0.007$	$k_{rT} = 0.027$
$k_{DT} = (0.37 \pm 0.03)$ dm^3 mol^{-1}	$k_D = 0.81 \pm 0.03$	

experimental fluorescence intensity vs pH data obtained in neutral-to-acid media were fitted with that equation. The good fits achieved (solid lines in Figure 2c−f) support the hypothesized mechanism, and the optimization process yielded the following values for the most significant parameters: $k_{CD}/k_C = 187 \pm 7$ dm^3 mol^{-1}, $k_{DT}/k_D = 0.46 \pm 0.05$, and $k_{TD}/k_T = 18 \pm 4$ dm^3 mol^{-1}. The first value indicates the great efficiency of the quenching of C* by protons. The two latter, which give information about the efficiency of the excited-state interconversion between species T* and D*, are roughly of the same order of those found for 4PBIQS.[3]

The fluorescence lifetimes measured at 380 nm are also in keeping with the proposed mechanism. As shown in Figure 1, only the species N* and C* contribute to the emission at that wavelength. At neutral pH species N* is responsible for the 380-nm emission and has a short lifetime of 0.2 ns. As the acidity is increased, the contribution of a second lifetime of 6.0 ns to the fluorescence decays becomes larger, while the percentage of the short component decreases. This is in good agreement with the variation of the concentrations of species C* and N* due to their ground-state acid−base equilibrium, the lifetime of 6.0 ns being attributable to species C*. It is interesting to note that this lifetime is much longer than that of the monocation C* of 2PBI under similar conditions (0.7 ns),[1] as expected from the fact that the concerted tautomerization C* → T* is rather efficient for 2PBI, whereas it is not detectable for 4PBI. The longer lifetime decreases with acidity at pH < 3, the plot of τ^{-1} versus proton concentration being linear (Figure 4a), as would be expected for the quenching of C* by protons to give D*. Furthermore, the good linearity of that plot supports the above statement that the reverse process, deprotonation of D* to give C*, does not take place. Fitting a straight line to the experimental lifetime data affords the following values: $(2.75 \pm 0.02) \times 10^{10}$ dm^3 mol^{-1} s^{-1} for the protonation rate constant k_{CD}, and 6.13 ± 0.02 ns for the lifetime of C* in the absence of quenching, the latter being in good agreement with the experimental lifetime of C* at low acidity. The value of k_{CD} is very close to the diffusion-controlled limit, as expected for such a process. These results allow calculation of the ratio $k_{CD}/k_C = 169$ dm^3 mol^{-1}, which agrees well with the value obtained above from the steady-state data.

When exciting at 349 nm only species T and D absorb, showing an isosbestic point at that wavelength. The fluorescence decays measured at 349-nm excitation and 520-nm emission therefore account for the time dependence of the fluorescence of species T* and D*. According to the proposed mechanism (Scheme 1), biexponential decays should be measured under those experimental conditions with lifetimes τ_1 and τ_2 depending on the pH and on the protonation, deprotonation and deactivation rate constants of species T* and D* as follows:[5]

$$(\tau_1,\tau_2)^{-1} = (^1/_2)\{(X + Y) \pm ((Y - X)^2 + 4k_{DT}k_{TD}[H^+])^{1/2}\} \quad (3)$$

$$X = k_T + k_{TD}[H^+] \quad (4)$$

$$Y = k_D + k_{DT} \quad (5)$$

However, all experimental decays were monoexponential with lifetimes decreasing as the concentration of protons increases, but whose reciprocal values do not follow the linear variation predicted by the Stern−Volmer equation for a single quenching process. This nolinearity indicates that both protonation of T* and deprotonation of D* take place in the excited state, and therefore the fact that only one exponential is experimentally observed may be due to the short lifetime of the second exponential -out of the limit of resolution of the lifetime spectrometer used- or to its very small amplitude.

To prove this interpretation, the function corresponding to τ_2 (minus sign in eq 3) was fitted to the experimental lifetimes at different acidities. Although the four parameters appearing in eqs 3−5 could be satisfactorily fitted, a strong correlation was found between k_{TD} and k_{DT}. Therefore, a constraint was introduced in the fit by fixing the ratio k_{DT}/k_D to the value obtained from the steady-state data (see above). The curve fitted under those conditions (solid line in Figure 4b) agrees very well with the experimental data, supporting our interpretation. From the values of the rate constants obtained in the fit (k_T, k_D, k_{DT}, and k_{TD} in Table 3), an intrinsic lifetime for T* of $\tau_T = 4.5 \pm 0.1$ ns is calculated that agrees well with the experimental value at pH 4, since at those acidities the concentration of protons is not high enough for the protonation of T* to take place, and the ratio $k_{TD}/k_T = 18 \pm 1$ dm^3 mol^{-1} is obtained, in very good agreement with that resulting from the fit of the steady-state data. The rate constants obtained allow us to predict the values of the second exponential, τ_1, at different acidities. By substituting the fitted parameters in the expression of τ_1 (eq 3 with plus sign), rather short values of τ_1 are obtained at any acidity (dashed line in Figure 4c). Furthermore, the amplitudes of the two theoretical exponentials can be estimated as a function of acidity by using the corresponding equations,[5] resulting in negative amplitudes for τ_1 whose absolute values are about 3 times smaller than those of τ_2 at high acidities and decrease to values of almost zero at low acidities. The coincidence of a short lifetime together with a small amplitude would explain our failure to observe the exponential of lifetime τ_1 under our experimental conditions.

The fluorescence quantum yields of species N*, C*, and T* together with their fluorescence lifetimes yielded the radiative deactivation rate constants of those species (Table 3). Furthermore, the ratio between the integrals of the contributions of T* and N* to the experimental emission spectrum at neutral pH, $R_{T/N} = 3.24$, can be shown to be $R_{T/N} = (k_{rT}/k_T)/(k_{rN}/k'_{NT})$. This expression allows the determination of the rate constant k'_{NT} for the photoinduced protonation of N* by water to give T*, $k'_{NT} = 2.7 \times 10^8$ s^{-1}, a value similar to those obtained for other aromatic amines.[7,19−21] Once k'_{NT} is known, the deactivation rate constant of species N*, k_N, can be calculated from the experimental lifetime of N* (Table 3). It must be noted that due to the effect of the medium observed at high acidities, the fluorescence quantum yield of D* varies with the concentration of $HClO_4$ or $NaClO_4$ and therefore its value has not been determined.

Acknowledgment. Part of the time-resolved fluorescence measurements presented in this work were made in the laboratory of Dr. Maçanita at the Structural Chemistry Centre in Lisbon, to whom we send our special thanks. This work was supported by the Xunta de Galicia (Project XUGA20906/B90

and the Infraestructura 1992 program) and by the DGICYT (Project PB90-0372 and postgraduate training grant awarded to M.N.).

References and Notes

(1) Rodríguez Prieto, F.; Mosquera, M.; Novo, M. *J. Phys. Chem.* **1990**, *94*, 8536.

(2) Novo, M.; Mosquera, M.; Rodríguez Prieto, F. *Can. J. Chem.* **1992**, *70*, 823.

(3) Novo, M.; Mosquera, M.; Rodríguez Prieto, F. *J. Chem. Soc., Faraday Trans. 2* **1993**, *89*, 885.

(4) Weller, A. *Prog. React. Kinet.* **1961**, *1*, 189.

(5) Ireland, J. F.; Wyatt, P. A. H. *Adv. Phys. Org. Chem.* **1976**, *12*, 131.

(6) Ormson, S. M.; Brown, R. G. *Prog. React. Kinet.* **1994**, *19*, 45. LeGourrierec, D.; Ormson, S. M.; Brown, R. G. *Prog. React. Kinet.* **1994**, *19*, 211.

(7) Arnaut, L. G.; Formosinho, S. J. *J. Photochem. Photobiol. A: Chem.* **1993**, *75*, 1. *J. Photochem. Photobiol. A: Chem.* **1993**, *75*, 21.

(8) It must be noted that a slight difference is observed between the two bands' excitation spectra, but that can be attributed to the presence of a very small concentration of species T at neutral pH , which becomes apparent due to the high fluorescence quantum yield of the excited species T*.

(9) Kondo, M. *Bull. Chem. Soc. Jpn.* **1978**, *51*, 3027.

(10) Brown, R. G.; Entwistle, N.; Hepworth, J. D.; Hodgson, K. W.; May, B. *J. Phys. Chem.* **1982**, *86*, 2418.

(11) Krishnamurthy, M.; Phaniraj, P.; Dogra, S. K. *J. Chem. Soc., Perkin Trans. 2* **1986**, 1917.

(12) Mishra, A. K.; Dogra, S. K. *Spectrochim. Acta* **1983**, *39A*, 609.

(13) Melhuish, W. H. *J. Phys. Chem.* **1961**, *63*, 229. Demas, J. N.; Crosby, G. A. *J. Phys. Chem.* **1971**, *75*, 991.

(14) Catalán, J.; Mena, E.; Fabero, F.; Amat-Guerri, F. *J. Chem. Phys.* **1992**, *96*, 2005.

(15) Amat-Guerri, F.; Catalán, J.; Mena, E.; Fabero, F. *Magn. Reson. Chem.* **1992**, *30*, 800.

(16) Eigen, M. *Angew. Chem., Int. Ed. Engl.* **1964**, *3*, 1.

(17) Note that the pH dependence of the T* emission band is the same as that of the N* emission band since the proton transfer process of rate k_{NT}' does not depend on the acidity.

(18) Novo Rodríguez, M. M. Procesos de transferencia protónica fotoinducida en 2-piridilbencimidazoles, Ph.D. Thesis; University of Santiago de Compostela, Spain, 1991.

(19) Favaro, G.; Mazzucato, M.; Masetti, F. *J. Phys. Chem.* **1973**, *77*, 601.

(20) Pines, E.; Huppert, D.; Gutman, M.; Nachliel, N.; Fishman, M. *J. Phys. Chem.* **1986**, *90*, 6366.

(21) Marzzacco, C. J.; Deckey, G.; Colarulli, R.; Siuzdak, G.; Halpern, A. M. *J. Phys. Chem.* **1989**, *93*, 2935.

JP950526J